Nuclear Instruments and Methods in Physics Research A 789 (2015) 43–49

Contents lists available at ScienceDirect

Nuclear Instruments and Methods in Physics Research A

journal homepage: www.elsevier.com/locate/nima

Tritiated water detection in the 2.17 μM spectral region by cavity ring down spectroscopy

C. Bray [a], A. Pailloux [b,*], S. Plumeri [c]

[a] CEA, DEN, DPC, F-91191 Gif-sur-Yvette, France
[b] CEA, DAM, DIF, F-91297 Arpajon, France
[c] Andra, 1-7 rue Jean Monnet, F-92298 Chatenay-Malabry, France

ARTICLE INFO

Article history:
Received 18 December 2014
Received in revised form
6 March 2015
Accepted 15 March 2015
Available online 3 April 2015

Keywords:
Nuclear waste containers
Infrared molecular spectroscopy
Continuous wave cavity ringdown spectroscopy (CRDS)
Radionuclide
HTO
Tritium detection

ABSTRACT

Nuclear waste containers are intended to be stored in dedicated disposal sites. For the inside and environmental safety of the disposal sites, the tiny outgassing rates leaking out the containers are measured. Presently, the radioactive HT gas is measured by liquid scintillation. However an alternative method—cavity ring down spectroscopy, an isotopically selective laser technique based on molecular spectroscopy—is currently developed and evaluated for tritium measurement in its oxidized form, HTO. Applying this method, the number density of the gaseous HTO sample hold in the optical cavity cell, is derived from the laser beam absorption by vibrational symmetric stretching $2\nu_1$ (R) HTO lines in the 4590 and 4600 cm^{-1} spectral range. To ensure a future accurate HTO measurement, the theoretical line intensities are confronted to the experiment: two tritiated water standards are measured with a dedicated CRDS set-up. Compared to the theoretical database, the line positions are correct (-0.067 to -0.128 cm^{-1}), their relative intensities are in agreement with the database, but their absolute intensities are 20% weaker. Among the seven intense lines, the 4596.485 cm^{-1} line (intensity 8.22 10^{-22} cm/molecule) and the 4592.407 cm^{-1} line (intensity 9.83 10^{-22} cm/molecule) are isolated and intense for a sensitive detection. The HTO detection limit with the present set-up is 3 kBq (10 min), equivalent to 1.8 10^{12} molecules in the 111 cm^3 CRDS cell. This detection limit could be improved by a factor 3 by reducing the detection noise.

1. Introduction

Nuclear wastes are classified according to the waste material, and their nuclear radiation type and activity. Various nuclear waste containers are designed to optimize the radionuclide confinement. Some groups of the air tight containers may release hydrogen or possibly small molecules or atoms (methane, carbon mono or dioxide, krypton) in scarce gas flow rate, below 10 l/container/year [1]. These gaseous species may include a small percentage of their radioactive isotope (HT, $^{14}CO_2$, $^{14}CH_4$, ^{85}Kr). In France, the medium activity long lived waste containers are intended to be stored in disposal sites. In order to ensure the safety of the facility and its environment, the outgassing of each container is characterized during the entrance acceptation procedure. Highly sensitive and selective methods are selected to measure these radioactive species. However, novel techniques are particularly welcomed if their application reduces the sampling period, improves the measurement. This paper focuses on the measurement of tritium, the radioactive isotope of hydrogen. Tritium is created by nuclear ternary fissions in the combustible, then migrates in the cladding and further. Tritium is then initially present in the related waste containers. Tritium is usually measured by liquid scintillation, after trapping the leaking HT and HTO in water. However, the gas sampling may last a few weeks to be measurable. Water is a well-known greenhouse gas, which strongly absorbs infrared radiation. Thus this paper proposes a laser absorption method based on vibrational molecular spectroscopy to quantify tritium in its oxidized form HTO.

CRDS, cavity ring down spectroscopy, measures molecular absorption spectra with sensitivity and high spectral resolution [2]. This technique is isotopically selective, real time (few minutes), and do not need calibration, if the spectroscopic parameters of the molecule are well known. The sample volume is small (few tens of cubic centimeters) and below atmospheric pressure, so sample having a small number of molecules is needed. Furthermore, CRDS is compact and cost-effective. This absorption technique sensitively measures molecules having a strong dipole, which is not the case of HT. Thus HT is first oxidized into HTO (with 100% efficiency), which has a strong rotation–vibration dipole. This study is the first stage of HTO measurement by CRDS, namely

* Corresponding author. Tel.: +33 1 69 26 40 00.
E-mail address: agnes.pailloux@cea.fr (A. Pailloux).

http://dx.doi.org/10.1016/j.nima.2015.03.064
0168-9002/

the intense and isolated rotation–vibration line selection in the theoretical database, the CRDS measurement of tritiated standards to experimentally retrieve the spectroscopic parameters of the HTO lines in the laser spectral region. The forthcoming absolute and accurate CRDS measurement relies on these spectroscopic parameters. Therefore, the theoretical parameters, modeled for this study, need an experimental assessment, and a comparison. The experiment also points out HTO lines interfered by isotopologues or pollutants; these lines may consequently be excluded for tritium detection. It also gives an evaluation the actual experimental set-up, then the directions for improvement.

2. Cavity ring down spectroscopy and HTO spectroscopy

The CRDS technique is detailed in the literature [2–4]. In this paragraph, only the important features are recalled. The beam of a single-mode continuous wave diode laser is injected, at a fixed frequency, in a high finesse cavity. A piezoelectric transducer moves back and forth one of the cavity mirrors in order to sweep the cavity length over at least one free spectral range, with a triangle modulation (30 Hz). This guaranties at least one resonance between the laser beam and the high finesse cavity within one period. When resonance occurs, the laser photons are progressively trapped inside the resonant cavity, accordingly producing an increased signal on the photodetector. Above a user defined threshold on the photodetector, the laser beam is promptly cut off by an acousto-optical modulator (AOM). The trapped photons then slowly decrease inside the cavity, either by absorption or by cavity losses; the resulting signal on the photodetector is an exponential decay which is measured and processed to determine the cavity lifetime, the so-called ring down time τ. The ring down time represents the overall cavity losses, including the molecular absorption of the gas sample inside the cavity. Precisely at a laser frequency ν, the ring down time $\tau(\nu)$ is a function of the gas sample molecular absorption coefficient $\alpha(\nu)$ (cm^{-1}), considering that the cavity losses generate a ring down time τ_0

$$\alpha(\nu) = \frac{1}{c}\left(\frac{1}{\tau(\nu)} \cdot \frac{1}{\tau_0}\right). \quad (1)$$

The molar concentration of a target species $[A]$ is classically derived from the absorption coefficient

$$\alpha(\nu) = [A] \cdot N \cdot \sigma(\nu) = [A] \cdot N \cdot S \cdot g(\gamma, \nu - \nu_0) \quad (2)$$

where $\sigma(\nu)$ is the molecular transition absorption cross-section (cm^2), N the molecular number density (cm^{-3}), proportional to the total gas pressure P and inversely proportional to the gas temperature T through the ideal gas law, and c is the speed of light (cm/s). Each molecular transition is characterized by its position ν_0, its intensity $S(T)$ in cm^{-1}/(molecule cm^{-2}), and a collisional broadening coefficient γ in cm^{-1}/atm (typically between 10^{-2} and 10^{-1} cm^{-1}/atm for self-collisions) and a Doppler (or temperature) broadening. The transition normalized profile $g(\gamma,\nu-\nu_0)$, typically modeled by a Voigt profile, is a function of the experimental conditions and the line spectroscopic parameters. No instrumental function is convoluted to the molecular line profile, considering the narrow laser linewidth. By a step by step laser frequency scanning, a CRDS spectrum measures the molecular lines absorption $\alpha(\nu)$; a few cm^{-1} wide spectrum is recorded within a few minutes.

If the spectroscopic parameters of the measured line are not well-known, standards are first measured to retrieve the spectroscopic parameters (intensities, positions and collisional broadening coefficients) from the absorption cross-section.

When the spectroscopic parameters (S, ν_0 and γ) are well-known, and the experimental parameters P and T are controlled, the molecular concentration of gas samples is derived from the measured absorption coefficient, which in turn is inversely proportional to the ring down time. As a consequence, no calibration is needed to measure the molecular concentration of a gas sample.

According to the literature, the rotation–vibration spectrum of HTO—line positions, intensities, broadening coefficients—is rarely studied. Helminger et al. [5] obtained pure rotational parameters using a high resolution microwave spectrometer. The references [6–9] give experimental data of the fundamental ν_1, ν_2 and ν_3 bands, using Fourier Transform Spectrometer or Tunable Diode Laser. More recently, Down et al. [10] theoretically analyzed the HTO transitions between 7200 and 7245 cm^{-1} using a spectra measured by Kobayashi et al. [11]. To our knowledge, no other harmonic band of HTO was studied with a high resolution spectroscopy technique.

The spectral region scanned by CRDS is generally limited to 15 cm^{-1} with one diode laser. Then, it is important to carefully

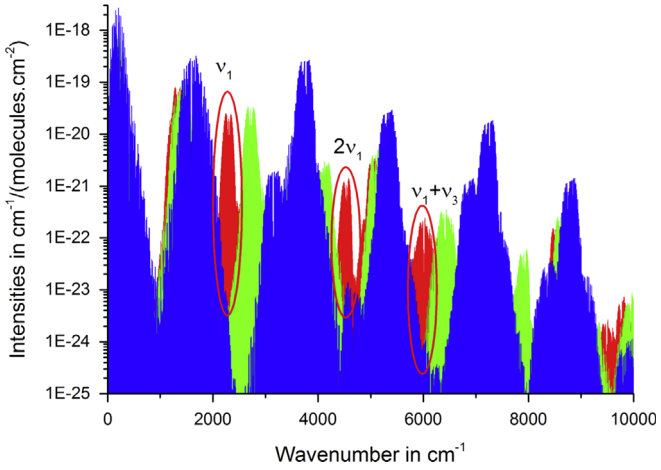

Fig. 1. Rotation–vibration transitions of water isotopologues, in the 0 and 10,000 cm^{-1} spectral region; $H_2^{16}O$, $H_2^{17}O$ and $H_2^{18}O$ (blue), HDO (green) and HTO (red). All these theoretical data are extracted from Spectra database [12]. (For interpretation of the references to color in this figure legend, the reader is referred to the web version of this article.)

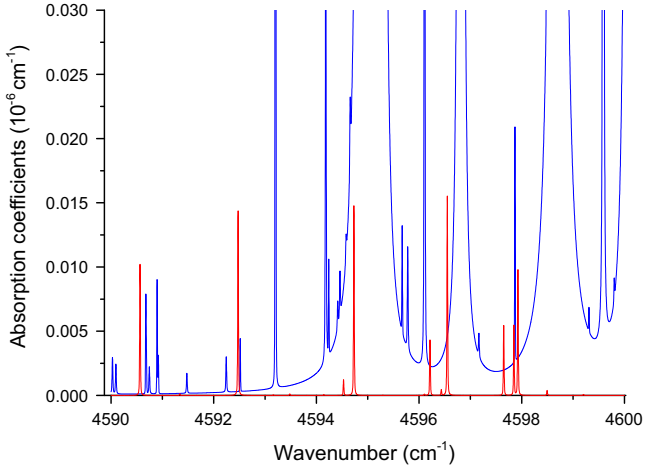

Fig. 2. Theoretical absorption spectra of 10 mbar pressure water stable isotopes $H_2^{16}O$, $H_2^{17}O$ and H_2^{18} and HDO (blue), with common isotopic abundance at 296 K [16]. The red line is the absorption spectra of 10^{-6} molar fraction of HTO [12]. (For interpretation of the references to color in this figure legend, the reader is referred to the web version of this article.)

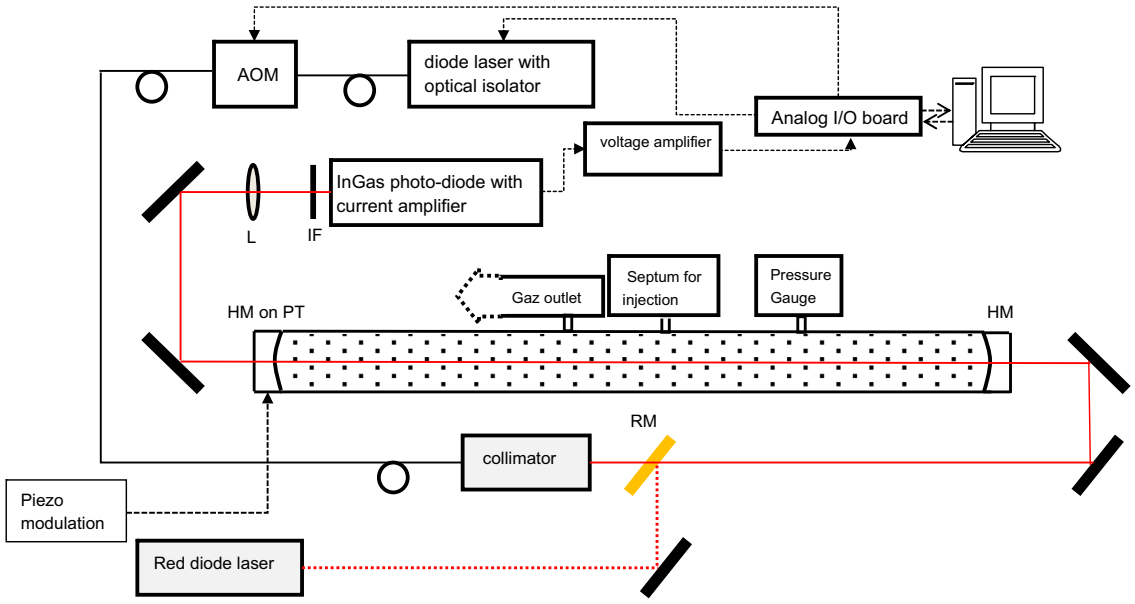

Fig. 3. CRDS experimental set-up for HTO measurement. The infrared laser beam is the red continuous line and the red dotted line is the red alignment laser beam. AOM stands for acousto-optical modulator, "RM" for removable mirror, "HM" for high reflectivity mirror, "PT" for piezoelectric transducer, "IF" for interferential filter, "L" for lens. (For interpretation of the references to color in this figure legend, the reader is referred to the web version of this article.)

Table 1
Name of the water standards, isotope composition and experimental condition for the spectra recorded in this work.

Standard name	Composition	Temperature in K	Pressure in mbar
Distilled water	$H_2^{16}O$: 99.73%, $H_2^{18}O$: 0.20%, $H_2^{17}O$: 0.037%, HDO: 0.031%	256 ± 1	25.02 ± 1.2
$H_2^{18}O$ enriched standard	$H_2^{16}O$: 2%, $H_2^{18}O$: 97.1%, $H_2^{17}O$: 0.9%	296 ± 1	26.21 ± 1.3
HDO enriched standard	H_2O: 85%, HDO: 15%	296 ± 1	26.94 ± 1.3
PerkinElmer 340 ± 4 MBq/g tritiated water standard	$H_2^{16}O$: 99.73%, $H_2^{18}O$: 0.20%, $H_2^{17}O$: 0.037%, HDO: 0.031%, HTO: $5.4\ 10^{-6}$	297 ± 1	28.35 ± 1.4
LNE 72 ± 0.21 MBq/g triated water standard	$H_2^{16}O$: 99.73%, $H_2^{18}O$: 0.20%, $H_2^{17}O$: 0.037%, HDO: 0.031%, HTO: $1.14\ 10^{-6}$	296 ± 1	26.53 ± 1.3

select the spectral region of the CRDS set-up dedicated to the HTO detection. An HTO transitions database is available [12]. The lines were calculated by Tashkun using PES [13] and DMS [14] and VTET computer code [15] with input parameters and basis adapted for this isotopologue. Fig. 1 represents the intensities of isotopologues of water transitions (H_2O, HDO and HTO) from 0 to 10,000 cm^{-1}. Three high intensities bands show up in the 0–10,000 cm^{-1} region, in the presence of water (H_2O and HDO). The ν_1 (symmetric stretching) fundamental band, centered at 2300 cm^{-1}, is the most intense band, but due to the cost and availability of the CRDS components in the mid-infrared, the $2\nu_1$, centered at 4500 cm^{-1}, is preferred. This HTO band is strong and reasonably isolated from other isotopologues. Strong and isolated HTO transitions of the $2\nu_1$ (R) band between 4590 and 4600 cm^{-1} are good candidates for the CRDS measurement of HTO. Fig. 2 shows the theoretical spectrum between 4590 and 4600 cm^{-1} of water with common isotopic abundance [16], containing 10^6 M fraction of HTO, for a total pressure of 10 mbar.

3. Experimental set-up and measurement protocol

The experimental set-up is presented on Fig. 3. A fibered Distributed Feed-Back diode laser, from Nanoplus®, centered at 2.172 μm (4592 cm^{-1}), produces the narrow linewidth laser beam. This diode laser is frequency tuned over a 8 cm^{-1} range by varying the diode temperature from 15 to 30 °C, the diode current being 100 mA, constant. The diode laser is control by the Newport 6100 controller, which has an uncertainty of ± 0.001 K° for temperature, and ± 0.01 mA for the intensity. An >30 dB optical isolator incorporated in the diode laser casing, suppresses the light reflexions toward the laser diode. The output power of the laser is about 3 mW, and the spectral linewidth is about 10 MHz at 4592 cm^{-1}. The laser beam propagates through the first order diffraction mode of an acousto-optical modulator (Brimrose® AMM-55-8-70-2200-2FP), which abruptly (50 ns) interrupts the laser beam, with a 50 dB efficiency, when the laser is resonant with the cavity. The Gaussian laser beam is mode matched with the fundamental cavity mode TEM_{00} with a lens: the waist diameter (583 μm) is adjusted and its position is centered between the 2 cavity mirrors. The laser beam is directed along the cavity axis by two flat mirrors. The cavity consists of two plano-concave high-reflectivity mirrors (Layertec®), having a 1 m radius of curvature. The quoted reflectivity of the mirror is greater than 0.9995 at 2.172 μm. The optical cavity is the measuring cell, containing the gas sample. The mirrors are located inside mirror mounts (LGR®), equipped with micrometers adjustment screws. The mirrors are vacuum-sealed with silicone o-rings. The mirrors are heated (a few degrees) by heating patches on the rear side, to avoid dew formation. Besides the mirrors and mirror mounts, the measuring cell is a stainless steel tube of 11 mm inner diameter; the total volume of the cell is 111 ± 13 cm^3. The cavity output is focused on a cooled InGaAs photodiode (Hamamatsu G5853-103). A homemade transimpedance amplifier circuit converts and amplifies the photodiode signal to a voltage signal. The signal is further amplified by a voltage amplifier (FEMTO DHPCA-100). The photodiode signal is connected to a fast (1.25 MHz) and 16 bit analog acquisition card (PCI-6111,

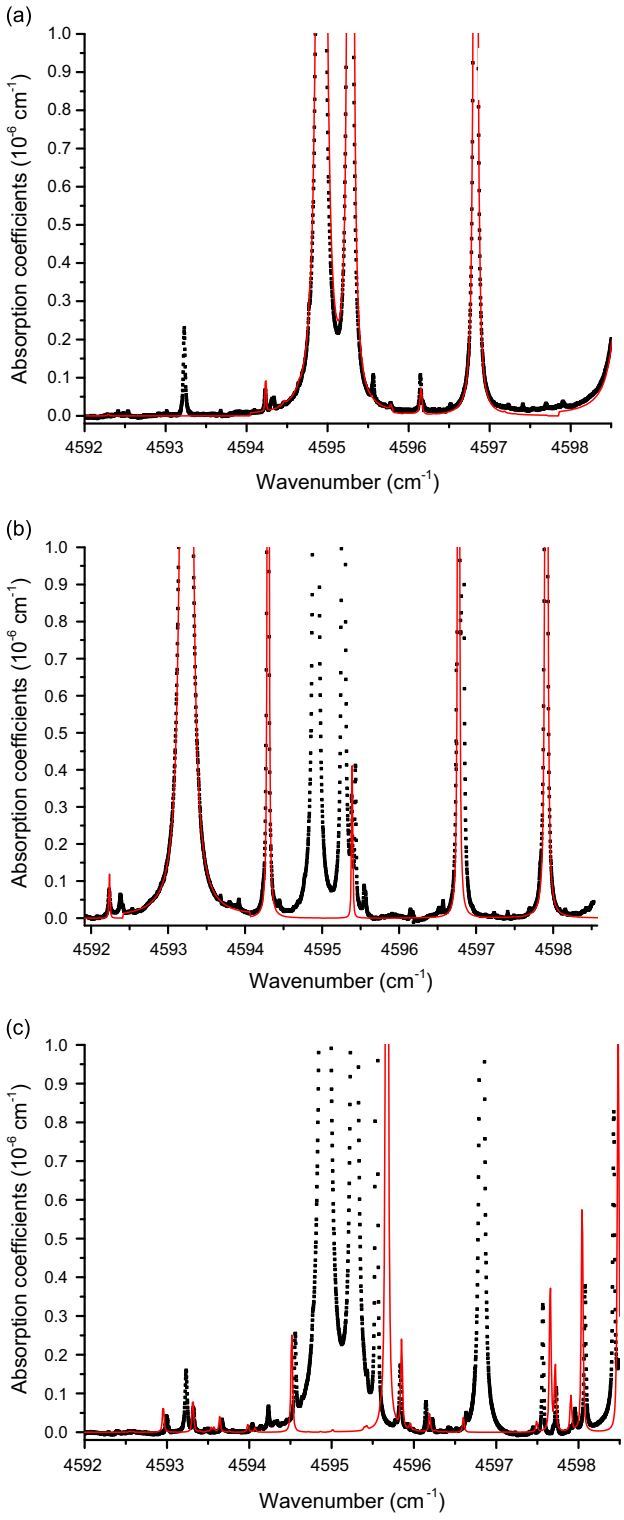

Fig. 4. Experimental (black dotted line) and theoretical (continuous red line) absorption spectra of (a) distilled water, (b) $H_2^{18}O$ enriched standard and (c) HDO enriched standard (Table 1). The theoretical spectra of $H_2^{16}O$, $H_2^{17}O$ and H_2^{18} are calculated using the HITRAN database [17], whereas the HDO and HTO spectra are calculated with the Spectra database [12].

National Instruments). The ring down time τ—typically 90–20 μs depending on molecular absorption—is evaluated by fitting the exponential laser decay, over a time range of seven lifetimes, by a Levenberg–Marquardt exponential fit.

The CRDS spectra are a succession of ring downs measured in a step by step mode, by changing the diode laser temperature with

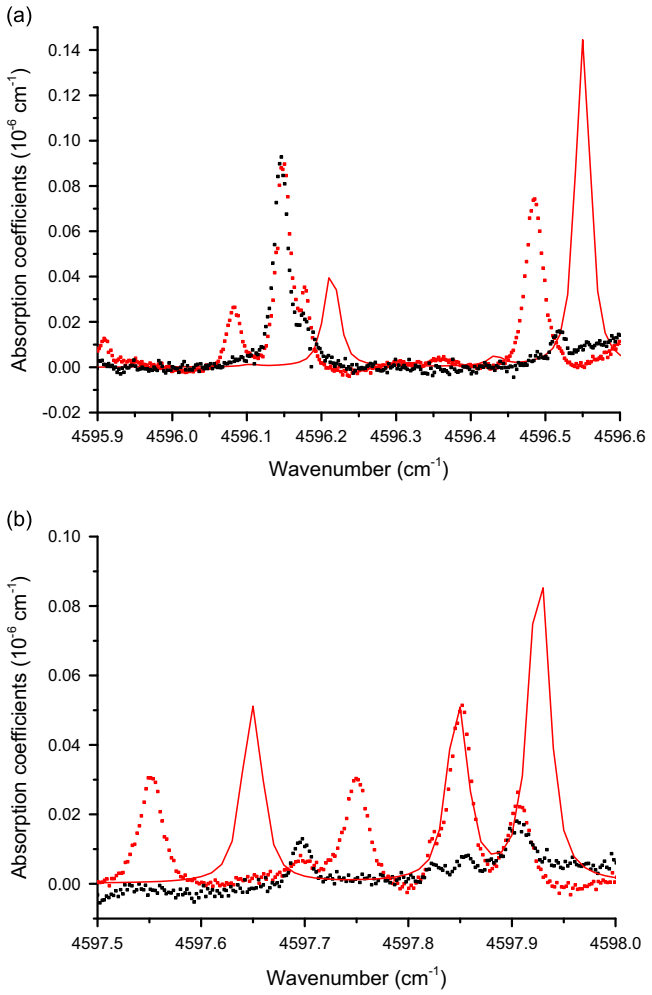

Fig. 5. Experimental (red dotted line) absorption spectra of the HTO enriched standard, with the theoretical (red continuous line) absorption spectra of HTO lines [12], and with the experimental (black dotted line) absorption spectra of distilled water. (For interpretation of the references to color in this figure legend, the reader is referred to the web version of this article.)

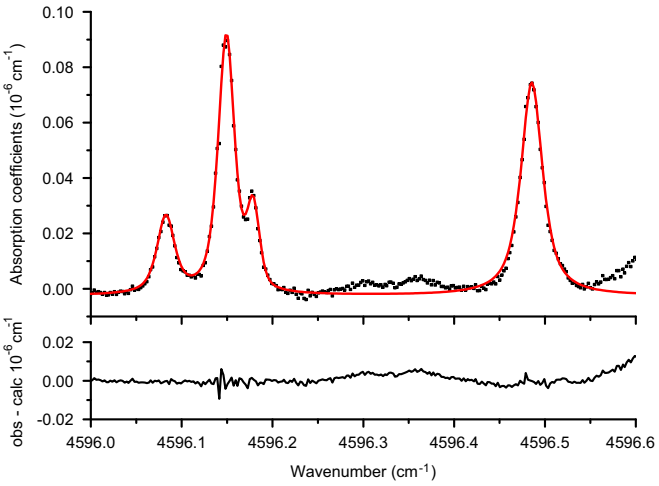

Fig. 6. Theoretical fit (red line) and residue (below) of 4 experimental (black dotted line) rotation–vibration transitions, measured with the Perkin Elmer HTO standard and a water vapor pressure of 28.35 mbar inside the CRDS cell. The 4596.083 and 4596.485 cm^{-1} transitions are two HTO transitions, the 4596.150 cm-1 line belongs to $H_2^{16}O$. Impurity lines rise around 4596.178 cm^{-1} and 4596.35 cm^{-1}. (For interpretation of the references to color in this figure legend, the reader is referred to the web version of this article.)

Table 2
Spectroscopic parameters of HTO transitions between 4592 and 4598 cm^{-1}. First column reports the transitions assignement. "Upper" stands for upper state of the transition, "band" for the vibrational band of the transition, and "Lower" for the lower state of the transition. Second column represents the experimental positions of the transitions given in cm^{-1}. Third column represents the theoretical positions of the transitions given in cm^{-1} from Schwenke/Partridge database [12]. Experimental (S) and theoretical (S_t) intensities are given in cm^{-1}/(molecule.cm^{-2}) at 296 K. γ represents the self-broadening coefficients (half-width at half-maximum) in cm^{-1}/atm.

Assignment			Position[a]	Position (theoretical)	S[b]	S_t	γ[c]
Upper	Band	Lower					
5 1 4	$2\nu_1$	4 1 3	4592.407	4592.475	1.08 10^{-21}[d]	1.159 10^{-21}	0.41
6 1 6	$2\nu_1$	5 1 5	4594.658	4594.731	9.58 10^{-22}	1.191 10^{-21}	0.43
6 4 3	$2\nu_1$	5 4 2	4596.083	4596.211	2.61 10^{-22}	1.851 10^{-22}	0.29
6 4 3	$2\nu_1$	5 4 1		4596.216		1.851 10^{-22}	
6 0 6	$2\nu_1$	5 0 5	4596.485	4596.550	9.09 10^{-22}	1.253 10^{-21}	0.40
6 3 4	$2\nu_1$	5 3 3	4597.552	4597.649	3.80 10^{-22}	4.403 10^{-22}	0.39
6 3 3	$2\nu_1$	5 3 2	4597.750	4597.848	3.04 10^{-22}	4.398 10^{-22}	0.31
6 2 5	$2\nu_1$	5 2 4	4597.824	4597.927	4.94 10^{-22}[d]	7.896 10^{-22}	0.28

[a] Line positions are estimated to be accurate to 0.001 cm^{-1}.
[b] Absolute linestrengths are estimated to be accurate to 15%.
[c] Self-broadening coefficients are estimated to be accurate to 30%.
[d] Small transition from impurities downgrades the accuracy of the measurement (20% for intensities and 35% for self-broadening coefficients).

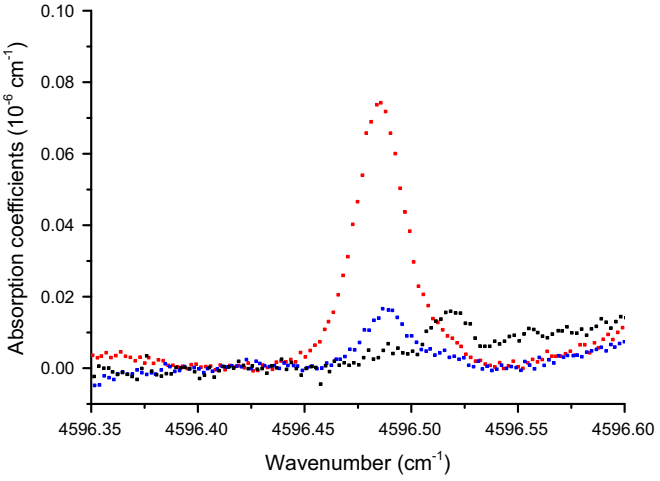

Fig. 7. Experimental absorption spectra of 3 water samples: the PerkinElmer tritiated water standard, 340 MBq/g (red dotted line), the LNE tritiated water standard, 72.21 MBq/g (blue doted line), and distilled water (black dotted line). An impurity line shows at 4596.54 cm^{-1} on the distilled water spectrum. (For interpretation of the references to color in this figure legend, the reader is referred to the web version of this article.)

an equivalent wavenumber step of 1.8 10^{-3} cm^{-1}. At each wavenumber, about 50 ring downs are averaged, leading to a noise equivalent absorption between 1.10^{-9} and 3.10^{-9} cm^{-1}. The laser beam wavenumber is calibrated by a wavemeter (HIGHFINESSE Wavelength Meter WS7, Ser. no 1270), with a 0.4 10^{-4} cm^{-1} accuracy.

Prior to a sample measurement, the cavity volume is pumped down by a turbo-molecular pump to about 10^{-4} mbar. The liquid

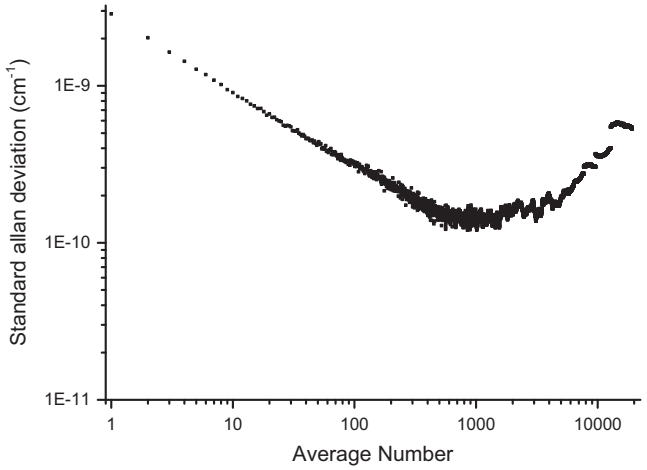

Fig. 8. Allan plot or the evaluation of the optimal ring down averaging using the present CRDS set-up.

water sample (a few μL) is injected in the cell through a septum (ThermoGreen®) using a chromatography syringe. The liquid instantly vaporizes, until vapor pressure is reached eventually. The cell pressure is monitored by a capacitance gauge (model 628D from MKS Instruments, 100 mbar full range, 373 K stabilized temperature, 0.25% accuracy of reading). All spectra are measured at room temperature, 22 ± 1 °C. The water vapor pressure is then 26.45 ± 0.16 mbar. Following the liquid sample injection, at least one hour is necessary to measure a stabilized gas pressure inside the cavity.

For safety reasons, the sample activity is limited to 2 MBq, hence small sample volumes are manipulated and even note worthier, the gas sample is measured in static condition, without gas circulation and permanent purification. Consequently, gaseous pollutants, produced by any outgassing from the cell, may slowly build up in the cavity. Indeed, impurities having vibrational bands in the studied spectral region are measured by CRDS. These pollutants are continuously released by O-rings polymers, when the water sample fills the cavity. Various polymers (ERIKS®) were unsuccessfully tested. To reasonably prevent the water transitions to be spectrally interfered by impurity lines, the CRDS spectra of water samples are measured one hour after the liquid injection. This delay is the best compromise between a completely stabilized gas pressure—related to water adsorption on the cell walls, driven by molecular diffusion—and a small partial pressure of impurities.

4. Results

4.1. Preliminary study: spectroscopy of the water stable isotopologues

The complex rotation–vibration spectrum of the water molecule is intensely studied in the frame of climate change. Water has 9 stable isotopologues. Therefore, a 10 cm^{-1} wide, high resolution and sensitive absorption spectrum of water theoretically shows tens of lines in our experimental conditions. On the other hand, the HTO concentration in the water sample is limited for safety reasons.

In order to identify unambiguously the HTO lines in a water sample, all the stable isotopologues lines showing in the 4590–4600 cm^{-1} region are first experimentally listed. To achieve this, a 97.1% $H_2^{18}O$ enriched standard, a 15% HDO enriched standard, and natural distilled water (Table 1) are measured successively by CRDS (Fig. 4) and compared theoretical spectra, modeled using the

international molecular databases [12,17]. The experimentally derived positions and intensities of $H_2^{16}O$, $H_2^{18}O$ and $H_2^{17}O$, are in good agreement with HITRAN database [17]. Compared to the "Spectra" database [12], the experimental HDO line positions are shifted between -0.13 and $0.05\ cm^{-1}$.

4.2. Tritiated water (HTO) measurement

As previously mentioned, the present measuring cell includes two polymer o-rings. Water molecules diffuse inside polymers. During the propagation through the polymer, tritium atoms may isotopically exchange with local hydrogen belonging to the polymer matrix. This dual process was clearly observed when measuring small volume samples containing a low concentration of tritium. A measuring cell without polymer should be designed for tritium quantification [18]. Meanwhile, spectroscopic studies are carried on by maintaining a saturated vapor pressure inside the measuring cavity; a small water reservoir is filled with the liquid sample to keep the gas phase in equilibrium with the liquid phase. Due to the H/T fractionation, the HTO concentration in the gas phase is slightly different from the concentration in the liquid phase. According to the literature, the HTO fractionation at 20 °C is about 0.91–0.92 [19–22]. Therefore the expected HTO concentration in gas phase is reduced by a 0.91 factor with respect to the HTO concentration in the liquid standard.

A tritiated water standard with 340.1 ± 4 MBq/g, or 5.7 ppm in molar fraction, (Table 1) was bought from PerkinElmer specifically for the HTO spectroscopic study. The HTO rotation–vibration spectrum is then measured by CRDS. No decrease of the mirror reflectivity is observed after an integrated four months exposure to 1 MBq. The HTO experimental spectrum (Fig. 5) is compared to the distilled water CRDS spectrum and to the HTO theoretical spectrum calculated using the "Spectra" database [12]. Seven HTO transitions are unambiguously identified in this 4592–4598 cm^{-1} spectral region. The CRDS spectrum is fitted using a MATLAB dedicated program to retrieve the intensity, position and broadening coefficient (HWHM) of each identified HTO line. Then the experimental HTO transitions are fitted (Fig. 6) with an easily computed Voigt profile with a calculated Doppler broadening. The experimental uncertainty of the line position is $10^{-3}\ cm^{-1}$. The uncertainty of the measured intensities is estimated to 16% with the following contributions: standard concentration 1.2%, influence of temperature in the determination of intensities 1%, pressure 5% (stabilization and air leak), fractionation of H/T 1%, fit 1% and experimental noise 5% (signal to noise ratio of 20). Traditionally, the broadening coefficient is accurately measured by varying the pressure. But the present set-up fixes the sample pressure to the vapor pressure; the resulting uncertainty of the self-broadening coefficient is therefore estimated to 30%. The spectroscopic parameters of the HTO transitions measured in the 4592–4598 cm^{-1} spectral region are summarized in Table 2. The experimental position of the HTO lines is shifted between -0.067 and $-0.128\ cm^{-1}$ from the theoretical position. The relative line intensities are in agreement with the theory. However, the measured intensities are 20% weaker than the theoretical (the H/T fractionation effect is already taken into account). This intensity discrepancy is further investigated by measuring another HTO standard: 72.21 ± 0.21 MBq/g, or 1.2 ppm (molar fraction), provided by the "Laboratoire national de métrologie et d'essais" (LNE). The intense and isolated $4596.485\ cm^{-1}$ HTO line is measured (Fig. 7) successively in the vapor pressure of the 340 ± 4 MBq/g PerkinElmer and the 72.21 ± 0.21 MBq/g LNE standards. The ratio of the measured line amplitudes is 4.7, consistent with the HTO concentration ratio in the standards. This additional result tends to confirm an overestimation of the theoretical intensities.

4.3. Evaluation of the HTO limit of detection

Two intense and isolated HTO transitions, studied previously, are selected for tritium detection: (514 $2\nu_1$(R) 413) $4592.407\ cm^{-1}$, and (606 $2\nu_1$(R) 505) $4596.485\ cm^{-1}$. An Allan-plot [23] was measured (Fig. 8) to determine the detection limit of the present experimental set-up, i.e. the optimized averaging N. The standard deviation of the noise decreases as $1/\sqrt{N}$ up to $N=600$ indicating a normal distribution of the noise. Considering an acquisition rate of 30 Hz, the limit of stability of the set-up is reach after 20 s. The Allan plot shows that the detection limit of the current CRDS set-up is $1.2\ 10^{-10}\ cm^{-1}$, when averaging 600 ring downs for each spectral data point. When averaging 50 ring downs (present experimental conditions), the CRDS detection limit is $5.5 \pm 0.8\ 10^{12}$ HTO molecules filled in a 111 cm^3 CRDS cell—or 9.8 ± 1.5 kBq —the laser beam being tuned to the $4596.485\ cm^{-1}$ transition. The CDRS measurement is completed within at 1 min.

5. Conclusion and perspective

This spectroscopy work of HTO is also a preliminary demonstration of tritium evaluation by CRDS, a laser absorption technique. The theoretically intense and isolated harmonic band of $2\nu_1$ (R) (symmetric stretching) between 4590 and $4600\ cm^{-1}$, is selected for this study. Although the water stable isotopologues $H_2^{16}O$, $H_2^{18}O$ and $H_2^{17}O$ have very weak lines in this spectral region, their position and intensity [17] are found in good agreement with the CRDS measurement. This was expected for this well-studied molecule. The experimentally measured positions of the HDO lines are slightly shifted from -0.13 to $+0.05\ cm^{-1}$ with respect to the "Spectra" database [12]. The seven HTO lines, unambiguously identified in the spectral range covered by the laser diode, are all slightly negatively shifted between -0.067 and $-0.128\ cm^{-1}$ with respect to the theory [12]. Their relative intensities are similar to the database, their absolute intensities are all about 20% weaker. These results show that the water molecular spectroscopy model is able to precisely predict the rotation–vibration spectra of water isotopologues.

According to this work, the CRDS techniques could measure HTO by scanning one or two intense and isolated HTO transitions: line 1, position $4592.407\ cm^{-1}$, intensity of $9.83\ 10^{-22}\ cm^{-1}$/molecule cm^{-2}, or line 2, position $4596.485\ cm^{-1}$, intensity of $8.22\ 10^{-22}\ cm^{-1}$/molecule cm^{-2}. Scanning the line 2, the actual set-up measures 9 kBq within 1 min, and the detection limit is 3 kBq, measured within 10 min, which corresponds to an optimized averaging of 600 per spectral data. Compared to other CRDS systems [24–26], the present CRDS set-up is noisier. By reducing the excess noise, mostly the electronic noise on detector, a 1 kBq detection limit is expected. This measurement capability matches the objective of this study; characterizing the tritium outgassing rate of a nuclear waste container, below 1 MBq/year, within a sampling period of a few days. Nevertheless, the key change to further quantify tritium applies on the CRDS measuring cell; polymers should be strictly prohibited, to prevent isotope exchange and the resultant tritium loss in the gas phase. Moreover, the gas phase could then be measured below vapor pressure, hence eliminating the H/T fractionation between the liquid and gas phases. Theses modifications are the identified next steps of the present study.

Acknowledgments

The authors thank Philippe Cassette from LNE for the fruitful discussions about tritium measurement and to supply the HTO

standard, Daniele Romanini, Alain Campargue and Samir Kassir from LIPhy (UMR 5588) for their constant support in developing CRDS technique and for the useful help concerning water molecular spectroscopy. They are also greatly thankful to CEA, DSV for giving access to the tritium laboratory in the frame a collaboration with CEA, DEN, DPC. This experimental study could start thanks to Guillaume Aoust's work on the CRDS set-up. This work was funded by the Agence nationale pour la gestion des déchets radioactifs (ANDRA).

References

[1] Synthesis report, National inventory of radioactive materials and waste, report number: 467VA, 2012, ⟨www.andra.fr⟩/.
[2] G. Berden, R. Engeln, Cavity Ring-Down Spectroscopy, Techniques and Applications, Wiley, Hoboken, NJ, USA, 2009.
[3] D. Romanini, K.K. Lehmann, Journal of Chemical Physics 99 (1993) 6287.
[4] D. Romanini, A.A. Kachanov, N. Sadeghi, F. Stoeckel, Chemical Physics Letter 264 (1997) 316.
[5] P. Helminger, F.C. De Lucia, W. Gordy, P.A. Staats, H.W. Morgan, Physics Review A 10 (1974) 1072.
[6] S.D. Cope, D.K. Russell, H.A. Fry, L.H. Jones, J.E. Barefield, Journal of Molecular Spectroscopy 127 (1988) 464.
[7] P.P. Cherrier, P.H. Beckwith, J.J. Reid, Molecular Spectroscopy 103 (1984) 41.
[8] G. Fayt, P.H. Steenbeckeliers, A. Kastler, Proceedings of the Academy of Science Paris. Series B 275 (1972) 459.
[9] O.N. Ulenikov., V.N. Cherepanov, A.B. Malikova, Journal of Molecular Spectroscopy 146 (1991) 97.
[10] M.J. Down, J. Tennyson, H. Masanori, Y. Hatano, K. Kobayashi, Journal of Molecular Spectroscopy 289 (2013) 35.
[11] K. Kobayashi, T. Enokida, D. Iio, Y. Yamada, M. Hara, Y. Hatano, Fusion Science and Technology 60 (2011) 941.
[12] ⟨http://spectra.iao.ru⟩/.
[13] H. Partridge, D.W. Schwenke, Journal of Chemical Physics 106 (1997) 4618.
[14] D.W. Schwenke, H. Partridge, Journal of Chemical Physics 113 (2000) 6592.
[15] D.W. Schwenke, Journal of Physics Chemistry 100 (1996) 2867.
[16] CRC, Handbook of Chemistry and Physics, 95th edition, CRC Press, W.M. Haynes, 2014.
[17] L.S. Rothman, I.E. Gordon, Y. Babikov, A. Barbe, D. Chris Benner, P.F. Bernath, M. Birk, L. Bizzocchi, V. Boudon, L.R. Brown, A. Campargue, K. Chance, L. Coudert, M.V. Devi, B.J. Drouin, A. Fayt, J-M. Flaud, R.R. Gamache, J. Harrison, J-M. Hartmann, C. Hill, J.T. Hodges, D. Jacquemart, A. Jolly, J. Lamouroux, R.J. LeRoy, G. Li, D. Long, C.J. Mackie, S.T. Massie, S. Mikhailenko, H.S.P. Müller, O.V. Naumenko, A.V. Nikitin, J. Orphal, V. Perevalov, A. Perrin, E.R. Polovtseva, C. Richard, M.A.H. Smith, E. Starikova, K. Sung, S. Tashkun, J. Tennyson, G.C. Toon, Vl.G. Tyuterev, J. Vander Auwera, G. Wagner, Journal of Quantative Spectroscopy and Radiative Transfer 130 (2013) 4.
[18] Y. Tang, S.L. Yang, K.K. Lehmann, Review of Scientific Instruments 83 (2012) 043115.
[19] O. Sepall, S.G. Mason, Canadian Journal of Chemistry 38 (1960) 2024.
[20] T.F. Johns, in: H. London (Ed.), Fractional Distillation and Solvent Extraction, Separation of Isotopes, George Newnes Books Ltd., London, 1961, pp. 41–94.
[21] D.G. Jacobs, 1968. Sources of tritium and its behavior upon release to the environment. Clearinghouse for Federal Scientific and Technical Information, National Bureau of Standards, U.S. Dept. of Commerce, Springfield.
[22] W.A. Van Hook, Journal of Chemical Physics 72 (1967) 1234.
[23] P. Werle, R. Mücke, F. Slerm, Applied Physics B. **57** (1993) 131.
[24] S. Kassi, I.E. Gordon, A. Campargue, Chemical Physics Letter 582 (2013) 6.
[25] A. Campargue, E.V. Karlovets, S. Kassi, Journal of Quantative Spectroscopy and Radiative Transfer 154 (2015) 113.
[26] A. Campargue, S. Kassi, D. Modelain, A. Barbe, E. Starikova, M.-R. De Backer, Vl.G. Tyuterev, Journal of Quantative Spectroscopy and Radiative Transfer 152 (2015) 84.